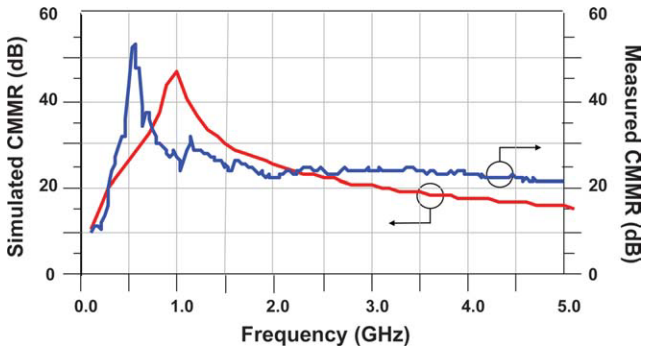

Figure 10 Comparison between simulated and measured CMRR. [Color figure can be viewed in the online issue, which is available at wileyonlinelibrary.com]

5. CONCLUSIONS

In this work, we studied high performances active baluns. Results showed that optimization of a differential amplifier coupling admittance enhances significantly the even mode rejection and allows approaching the theoretical optimal admittance. It was confirmed by measurements. Moreover, a complementary optimization is needed to associate high CMRR and a good noise figure (input balun) or IP3 point (output balun).

ACKNOWLEDGMENTS

The authors thank S. Kovacic and H. Lafontaine for their technical help.

REFERENCES

1. Y.J. Yoon, Y. Lu, R.C. Frye, M.Y. Lau, P.R. Smith, L. Ahliquist, and D.P. Kossives, Design and characterization of multilayer spiral transmission-line baluns, IEEE Trans Microwave Theory Tech 47 (1999), 1481–1487.
2. A.H. Baree and I.D. Robertson, Monolithic MESFET distributed baluns based on the distributed amplifier gate-line termination technique, IEEE Trans Microwave Theory Tech 45 (1997), 188–195.
3. M. Kawashima, T. Nagakawa, and K. Araki, A novel broadband active balun, In: European Microwave Conference, Munich, 2003.
4. K. Jung, W.R. Einsenstadt, R.M. Fox, A.W. Ogden, and J. Yoon, Broadband active balun using combined cascade-cascade configuration, IEEE Trans Microwave Theory Tech 56 (2008), 1790–1796.
5. Y. Xuan and J.L. Fikart, Computer-aided design of microwave frequency doublers using a new circuit structure, IEEE Trans Microwave Theory Tech 41 (1993), 2264–2268.
6. H. Ma, Novel active differential phase splitters in RFIC for wireless applications, IEEE Trans Microwave Theory Tech 46 (1998), 2597–2603.
7. F. Centurelli, R. Luzzi, P. Marietti, G. Scotti, P. Tommasino, and A. Trifiletti, An active balun for high-CMRR IC design, In: 13th GAAS Symposium, 2005, pp.621–624.
8. C. Viallon, E. Tournier, J. Graffeuil, and T. Parra, An original SiGe active differential output power splitter for millimetre-wave applications, In: European Microwave Conference, Munich, 2003.
9. J. Gonzalez, B. Delacressonnière, J.-L. Gautier, and I. Telliez, Déphaseur actif 180° large bande, In: Journées Nationales Micro-ondes, Brest, 1993.
10. F. Temcamani, P. Lida, B. Delacressonnière, and J.-L. Gautier, Limitations of the even mode rejection in differential structures, In: European Microwave Conference, Madrid, 1993.
11. T. Khelifi, J.-L. Gautier, and E. Bourdel, Structures différentielles à TBH et applications, In: ANTEM 96, Montréal, 1996.

AN EMPIRICAL *I-V* NONLINEAR MODEL SUITABLE FOR GAN FET CLASS F PA DESIGN

A. García-Osorio,[1] J. R. Loo-Yau,[1] J. A. Reynoso-Hernández,[2] Susana Ortega-C.,[1] and J. L. del Valle-Padilla[1]

[1] Centro de Investigación y Estudios Avanzados del I. P. N. Unidad Guadalajara, Av. Científica 1145, Colonia El Bajío, C. P. 45015, Zapopan, Jalisco, México; Corresponding author: rloo@gdl.cinvestav.mx

[2] Centro de Investigación Científica y Estudios Superiores de Ensenada, Carretera Ensenada Tijuana 3918, Zona Playitas, C. P. 22860, Ensenada, B. C., México

Received 30 August 2010

ABSTRACT: *This article presents an improved nonlinear* $I_{DS}(V_{GS}, V_{DS})$ *model useful for modeling the experimental pulsed* I-V *measurement data of GaN FETs operated at large drain-source voltages. This improved* $I_{DS}(V_{GS}, V_{DS})$ *model is based on the Chalmers model. The main features of the improved nonlinear* $I_{DS}(V_{GS}, V_{DS})$ *model are the two analytical expressions that are incorporated to model the output conductance and the saturation voltage. The new model only requires 13 parameters easily determined from experimental pulsed* I-V *data. Comparison between simulated and measured data of an inverse class F PA designed with a commercial GaN FET at 1.5 GHz demonstrate that the proposed model is suitable for microwave circuit design based on GaN transistors.* © 2011 Wiley Periodicals, Inc. Microwave Opt Technol Lett 53:1256–1259, 2011; View this article online at wileyonlinelibrary.com. DOI 10.1002/mop.25980

Key words: *GaN FET; nonlinear model; Chalmers model; class F PA*

1. INTRODUCTION

The heterojunction field effect transistor based on AlGaN/GaN is a good candidate for high-power microwave frequencies applications, for example in high efficiency power amplifiers (class B, F, and E) as well as for high-linearity power amplifiers (class A). Thus, to design high efficiency and high linearity power amplifiers, accurate nonlinear equivalent circuit models for AlGaN/GaN HEMT are required. Figure 1 shows the nonlinear equivalent circuit of an AlGaN/GaN and it consists of intrinsic nonlinear elements and extrinsic or parasitic linear elements.

To obtain a nonlinear model suitable for GaN FETs modeling, the first step is to guarantee that the *I-V* characteristics of the FET can be modeled with high accuracy. In that sense, the Chalmers model [1] seems to be a good candidate for GaN modeling due to its characteristics, simplicity, and high accuracy already demonstrated in GaAs FET. The second step is to model

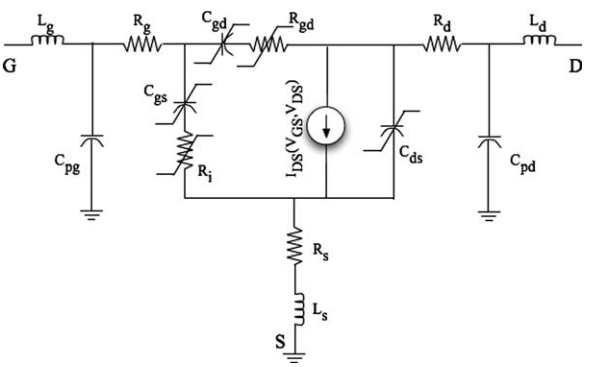

Figure 1 Nonlinear GaN FET electrical equivalent circuit

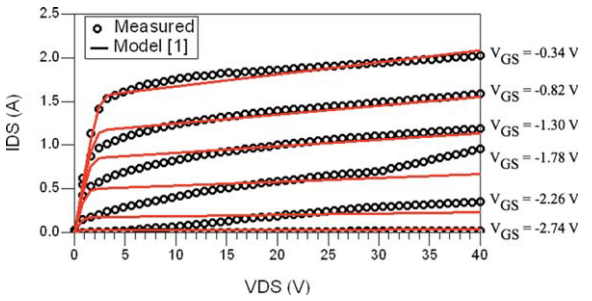

Figure 2 Pulsed *I-V* of the CGH35015 packaged GaN FET. [Color figure can be viewed in the online issue, which is available at wileyonlinelibrary.com]

the nonlinear behavior of the intrinsic elements of the FET as C_{gs}, C_{gd}, C_{ds}, R_i, and R_{gd}, where C_{gs} and C_{gd} are the most significant nonlinear elements, after the current $I_{DS}(V_{GS}, V_{DS})$. In addition, the models of $I_{DS}(V_{GS}, V_{DS})$ and the capacitances have to satisfy the current and charge conservation law to avoid nonconvergence problems in harmonic balance simulations [2].

In practice, as already pointed out in [3], the Chalmers model does not successfully predicts the pulsed *I-V* characteristics of GaN FETs operated under large drain-source voltages. Thus, a modification to the Chalmers model was proposed in [4]. This modification allows for the dispersion of both the transconductance (g_m) and the conductance (g_{ds}). However, the main limitation in [3] and [4] is the lack of information to determine the initial values of the parameters to feed the model.

Based on [1], an improved nonlinear $I_{DS}(V_{GS}, V_{DS})$ model useful for predicting the pulsed *I-V* experimental data of GaN FETs operated at large drain-source voltages is presented. The improved model uses the basic structure of [1] along with two analytical expressions to model the output conductance and the saturation voltage as a function of V_{GS}, as proposed by Tanimoto [5].

The proposed model was used to design an inverse class F PA at 1.5 GHz. The simulation results for power added efficiency (PAE), gain and output power fit properly the measured data, demonstrating the usefulness of the proposed model for microwave PAs design.

2. THE *I-V* MODEL

According to [1], the *I-V* characteristics of microwave FETs can be predicted by

$$I_{DS}(V_{GS}, V_{DS}) = I_{pk}(1 + \tanh(\psi))(1 + \lambda V_{DS}) \tanh(\alpha V_{DS}), \quad (1)$$

where,

$$\psi = P_1(V_{GS} - V_{pk}) + P_2(V_{GS} - V_{pk})^2 + P_3(V_{GS} - V_{pk})^3. \quad (2)$$

I_{pk} and V_{pk} are the drain current and gate to source voltage, respectively, at the maximum g_m; λ represents the output conductance and α represents the saturation voltage.

In general, (1) describes quite well the pulsed *I-V* characteristics of on-wafer GaN FETs. However, in several available commercial packaged GaN FETs, the Chalmers model is not suitable to predict the experimental data at large V_{DS}, when V_{GS} is close to V_{TH} as shown in Figure 2. At large V_{DS}, the output conductance (λ) and the saturation voltage (α) are nonlinear function of V_{GS}.

To improve the performance of (1), λ and α have to be modeled with appropriate functions that describe its behavior. Thus, based on [5], the analytical expression used to predict the behavior of λ and α, as a function of V_{GS}, can be written as:

$$\lambda(V_{GS}) = \lambda_3 - \lambda_0(1 + \lambda_1 V_{GS}) \tanh(\lambda_2 V_{GS}), \quad (3)$$

$$\alpha(V_{GS}) = \alpha_0 + \alpha_1 e^{-\left(\frac{V_{GS} - \alpha_2}{\alpha_3}\right)^2} \quad (4)$$

where λ_0, λ_1, λ_2, λ_3, α_0, α_1, α_2, and α_3 are parameters that can be determined directly from the pulsed *I-V* measured data. A procedure to extract these parameters is presented in Section 3. The modification implies the determination of 13 parameters instead of 7 or 11 parameters as in [1, 4] and [6], respectively.

Notice that the proposed model still uses the basic core of [1], thus the current conservation law [2] is satisfied.

3. EXTRACTION OF THE *I-V* MODEL

The initial values of the parameters in (1) and (2), I_{pk}, V_{pk}, P_1, P_2, and P_3 can be determined as proposed in [7]. Thus, in this article, we only describe the procedure to determine the initial values for the parameters of (3) and (4).

The dependance of λ and α with respect to V_{GS} is determined by modeling the drain-to-source current, for a constant V_{GS}, according to:

$$I_{DS}(V_{DS}) = I_{max}(1 + \lambda(V_{GS})V_{DS}) \tanh(\alpha(V_{GS})V_{DS}) \quad (5)$$

where I_{max} represents the maximum drain-source current, λ can be determined from the slope of the drain-source current in the saturation region, and α is the 65% of the knee voltage [8]. Notice that λ and α must be determined for every single V_{GS}.

Once $\lambda(V_{GS})$ and $\alpha(V_{GS})$ are known, the parameters λ_i ($i = 0, 1, 2, 3$) and α_j ($j = 0, 1, 2, 3$) from (3) and (4), respectively, are calculated by means of a nonlinear least square method using the curve fitting toolbox of MATLAB(R). Figure 3 compares the pulsed *I-V* data (measured with a Dynamic *I-V* Analyzer DiVA265) of the GaN FET CGH35015 from Cree with the proposed model. The results demonstrate that the proposed model has a high correlation with the experimental *I-V* data. Moreover, Figure 4 shows experimental and modeled data of the output conductance at different V_{GS}, whereas Figure 5 compares the model with the experimental data of the transconductance as well as with the first derivative of the transconductance at different V_{DS}.

It is important to comment that all the parameters of the improved model are determined ignoring the parasitic resistances. This means that all the parameters of the improved model are referenced to the extrinsic voltage instead of the intrinsic voltage. This problem is presented in most of the *I-V* empirical

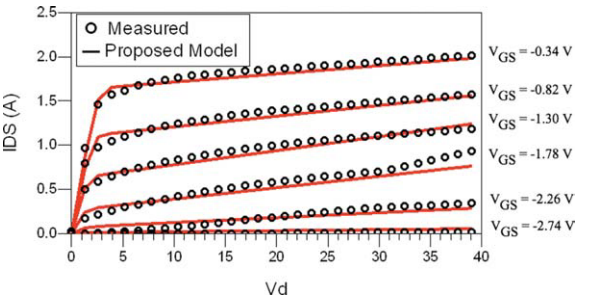

Figure 3 Pulsed *I-V* of the CGH35015 using the proposed model. [Color figure can be viewed in the online issue, which is available at wileyonlinelibrary.com]

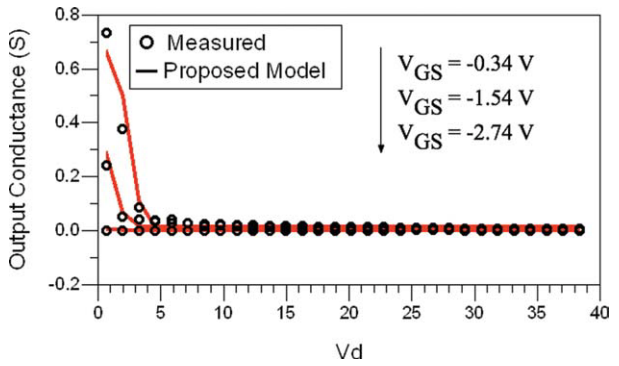

Figure 4 Output conductance of the CGH35015 modeled with the proposed model. [Color figure can be viewed in the online issue, which is available at wileyonlinelibrary.com]

nonlinear models. Therefore, to overcome this problem, a final optimization routine using ADS(R) was performed.

4. VALIDATION OF THE MODEL

The model was validated with the design of a 1.5 GHz inverse class F PA using an available commercial packaged GaN FET RT233PD from RFHIC. The values of the parameters of the proposed *I-V* model are reported in Table 1. In addition, the parasitic elements were extracted using the method proposed in [9] and [10], whereas the intrinsic elements were determined using the method proposed in [11].

An inverse class F PA is a high-efficiency power amplifier. The main characteristic of the inverse class F PA lies in the voltage and current waveform at the drain of the FET. Basically, the idea behind of an ideal inverse class F PA is to produce a half wave sinusoid signal voltage in the drain, whereas the current has to be a square signal. Both voltage and current signal have to be 180° out of phase. Under this condition, the inverse class F PA can reach 100% of drain efficiency. To obtain the ideal waveform of the inverse class F PA, it is necessary to determine the optimum output impedance at the fundamental frequency, whereas high and low output impedance have to be presented at even and odd harmonics, respectively. This task is very difficult to achieve. However, Raab [12] demonstrates that a drain efficiency greater than 75% can be obtained, just considering the fundamental frequency and the second and third harmonic. Hence, input and output impedance of the inverse class F PA were determined by means of a harmonic load and source pull simulation using the proposed nonlinear model on ADS(R).

The output matching network is based on the topology presented in [13]. The physical dimensions of the microstrips were optimized to achieve the highest PAE at 1.5 GHz with an input power of 23 dBm and with an input matching network designed at S_{11} complex conjugated. Once the output matching network was optimized, a harmonic source pull simulation was performed to obtain the appropriate input impedance needed to synthesize the correct input matching network under the same condition of frequency and input power. Input and output impedances of the inverse class F PA are reported in Table 2. Notice that for both matching networks, input and output, the impedances are high and low, respectively, for the second and third harmonic as required for an inverse class F PA.

Based on the information in Table 2, the input and output matching networks were fabricated on a FR4 substrate with a $\varepsilon_r = 4.25$ and $h = 0.034$ mm, and external bias tees from Picosecond Pulse Lab model 5580 were used. The inverse class F PA was biased with a $V_{GS} = -2.3$ V and $V_{DS} = 10$ V. Figure 6 demonstrates that at 23 dBm of input power, the drain voltage waveform can be approximated to a half sinusoid, whereas the drain current waveform is similar to a square waveform.

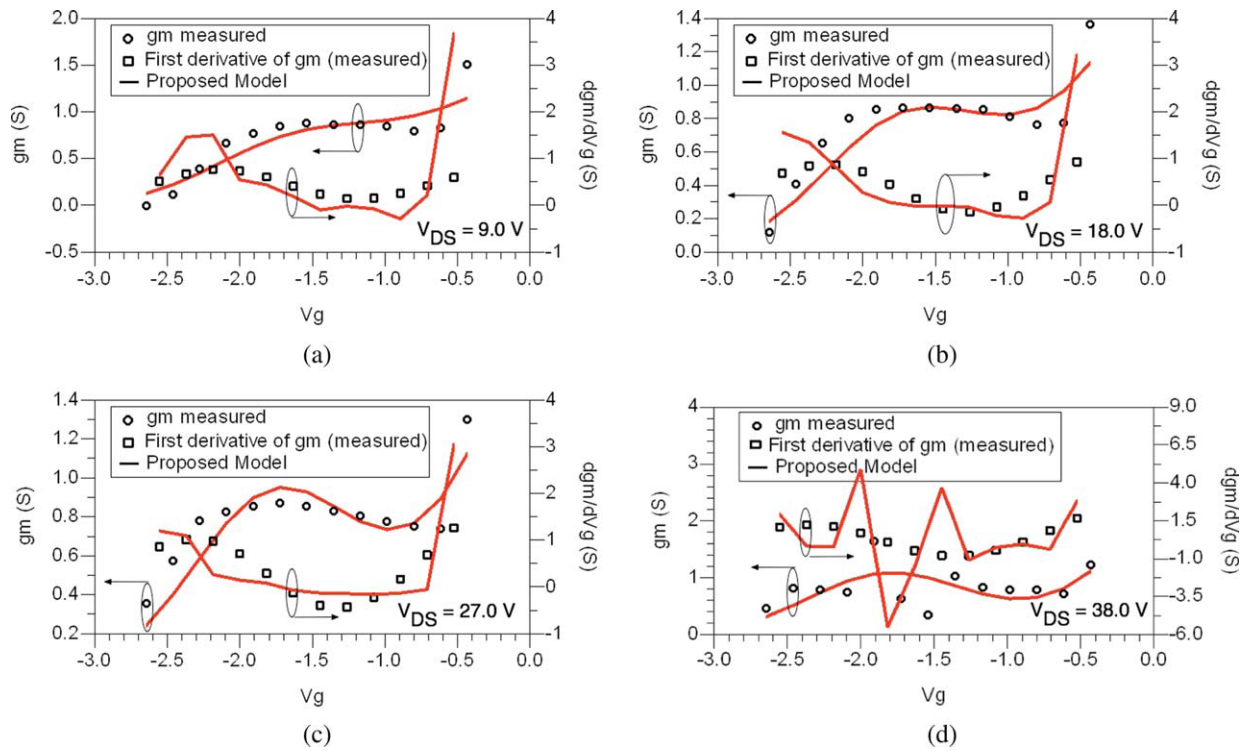

Figure 5 Transconductance of the CGH35015 modeled with the proposed model: (a) $V_{DS} = 9.0$ V, (b) $V_{DS} = 18.0$ V, (c) $V_{DS} = 27.0$ V, and (d) $V_{DS} = 38.0$ V. [Color figure can be viewed in the online issue, which is available at wileyonlinelibrary.com]

TABLE 1 Parameters of the Proposed Model for the RT233PD

I_{pk} (A)	V_{pk} (V)	P_1 (1/V)	P_2 (1/V^2)	P_3 (1/V^3)
0.696	−1.453	1.315	0.061	0.478
λ_0 (1/V)	λ_1 (1/V)	λ_2 (1/V)	λ_3 (1/V)	
19.248	0.601	−0.002	0.015	
α_0 (1/V)	α_1 (1/V)	α_2 (V)	α_3 (V)	
−1.355	0.123	−1.366	0.198	

TABLE 2 Input and Output Impedances of the Inverse Class F

	Z (f_0) Ω		Z ($2f_0$) Ω		Z ($3f_0$) Ω	
	Magnitude	Phase	Magnitude	Phase	Magnitude	Phase
Input	10.97	−80.15°	26.17	−76.67°	2.71	−72.20°
Output	20.58	−4.54°	30.36	−68.78°	6.87	6.32°

Figure 7 compares the measured and simulated output power, transducer gain and PAE of the inverse class F PA, designed with the GaN RT233PD. The simulation results show a high correlation with the experimental data.

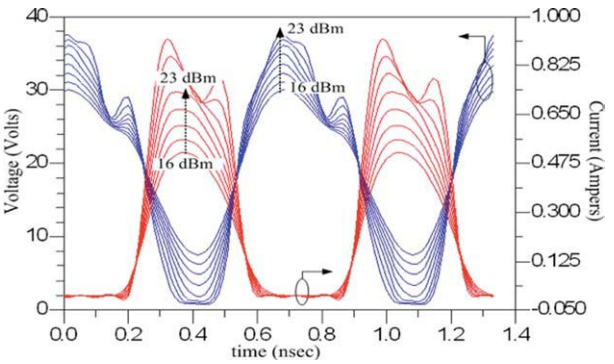

Figure 6 Voltage and current waveform of the class F PA at different input power. [Color figure can be viewed in the online issue, which is available at wileyonlinelibrary.com]

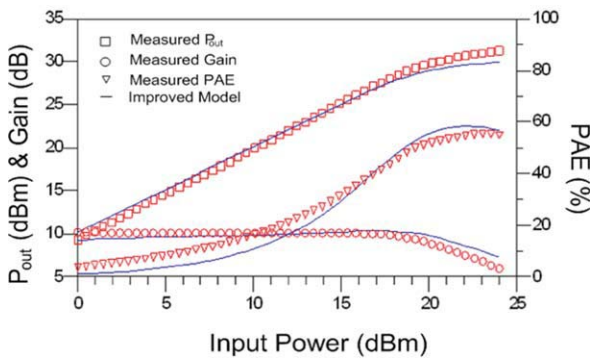

Figure 7 Output power, gain, and PAE of the inverse class F PA. [Color figure can be viewed in the online issue, which is available at wileyonlinelibrary.com]

5. CONCLUSIONS

This article introduced an improved compact analytical model to predict the pulsed *I-V* experimental data of GaN HEMTs operated under large drain-source voltages. In addition, it is shown that the ohmic region of the HEMTs can be modeled with high accuracy. These two features are achieved thanks to the two analytical expressions used to predict the nonlinear behavior of the output conductance and the saturation voltage as a function of V_{GS}. Moreover, the improved model can predict the gate-source dependence of the output conductance as well as to predict the transconductance g_m of GaN HEMTs operated at large drain-source voltages. The improved model requires 13 parameters that can be determined directly from experimental data.

The improved model has been used to evaluate the performance of an inverse class F power amplifier. The output power, gain, and PAE have been predicted by the nonlinear model and confirmed by experimental data.

REFERENCES

1. I. Angelov, H. Zirath, and N. Rorsman, A new empirical model for HEMT and MESFET devices, IEEE Trans Microwave Theory Tech 40, (1992), 2258–2266.
2. D. Root and B. Hughes, Principles of nonlinear active device modeling for circuit simulation, In: 32nd Automatic Radio Frequency Techniques Group, 1988.
3. P.M. Cabral, J.C. Pedro, and N. Borges, New nonlinear device model for microwave power GaN HEMTs, In IEEE International Microwave Symposium, Fort Worth, TX, 2004, pp. 51–54.
4. I. Angelov, V. Desmaris, K. Dynefors, et al., On the large signal modeling of AlGaN/GaN HEMTs and SiC MESFET, In: 13th GAAS Symposium, 2005, pp. 309–312.
5. T. Tanimoto, Analytical nonlinear HEMT model for large signal circuit simulation, IEEE Trans Microwave Theory Tech 44 (1996), 1584–1596.
6. C. Fager, J.C. Pedro, N.B. Carvalho, and H. Zirath, Prediction of IMD in LDMOS transistor amplifiers using a new large signal model, IEEE Trans Microwave Theory Tech 50 (2002), 2834–2842.
7. J.R. Loo-Yau, J.A. Reynoso-Hernandez, J.E. Zuñiga-Juarez, et al., Modeling I-V characteristic of the power microwave FET with the Angelov model using pulse measurements, Microwave Opt Technol Lett 48 (2006), 1046–1050.
8. Y.C. Chen, D.L. Ingram, H.C. Yen, R. Lai, et al., A new empirical I-V model for HEMT devices, IEEE Microwave Guided Wave Lett 10 (1998), 342–344.
9. A. Zarate de Landa, J.E. Zuñiga-Juarez, J.A. Reynoso-Hernandez, et al., A new and better method for extracting the parasitic elements of on-wafer GaN transistors, In: IEEE International Microwave Symposium, Honolulu, HI, 2007, pp. 791–794.
10. J.A. Reynoso-Hernández, J.R. Loo-Yau, J.E. Zuñiga-Juárez, et al., A straightforward method to determine the parasitic gate resistance of GaN FET, In: IEEE International Microwave Symposium, Boston, 2009.
11. M. Berroth and R. Bosch, Broadband determination of the FET small signal equivalent circuit, IEEE Trans Microwave Theory Tech 38 (1990), 891–895.
12. F.H. Raab, Class-F power amplifiers with maximally flat waveforms, IEEE Trans Microwave Theory Tech 45 (1997), 2007–2012.
13. Y.Y. Woo, Y. Yung, and B. Kim, Analysis and experiments for high efficiency class F and inverse class F power amplifiers, IEEE Trans Microwave Theory Tech 54 (2006), 1964–1974.